Wireless Pers Commun (2014) 78:449–474
DOI 10.1007/s11277-014-1761-8

QoS-Driven Power Allocation Under Peak and Average Interference Constraints in Cognitive Radio Networks

Stavroula Vassaki · Marios I. Poulakis · Athanasios D. Panagopoulos · Philip Constantinou

Published online: 10 April 2014

Abstract Efficient radio spectrum utilization can be improved using cognitive radio technology. In this work, we consider a spectrum underlay cognitive radio system operating in a fading environment. We propose an efficient power control scheme that maximizes the effective capacity of the secondary user, provisioning quality of service while on the same time the communication of the primary user is guaranteed through interference constraints. The specific power allocation scheme uses a policy in which the outage events of the primary user are exploited leading to a significant increase of the secondary user's effective capacity. Moreover, the interference of the primary link to the secondary is taken into account so as to study a more realistic scenario. In order to safeguard primary user's communication, two types of restrictions are considered: the traditional interference power constraint and the proposed inverse signal to interference plus noise ratio constraint. Different scenarios depending on the nature of the constraints (peak/average) are studied and their impact on the performance of the primary and secondary users is investigated. The superiority of the proposed schemes is demonstrated through their comparison with two reference power control schemes. Finally, numerical calculations, validated with simulation results, confirm the theoretical analysis and evaluate the performance of the proposed scheme for all the different scenarios.

Keywords Power allocation · Cognitive radio · Interference constraints · Effective capacity

S. Vassaki (✉) · M. I. Poulakis · A. D. Panagopoulos · P. Constantinou
School of Electrical and Computer Engineering, National Technical University of Athens, Iroon Polytexneiou 9, Athens, Greece
e-mail: voula@mobile.ntua.gr

M. I. Poulakis
e-mail: marios@mobile.ntua.gr

A. D. Panagopoulos
e-mail: thpanag@ece.ntua.gr

P. Constantinou
e-mail: fkonst@mobile.ntua.gr

1 Introduction

The main characteristic of next generation wireless networks is the increasing spectral requirements. The satisfaction of these demands may induce congestion in the scarce spectral resource, whereas on the same time its utilization through the traditional allocation techniques remains inefficient [1,2]. Considering these problems, the researchers have introduced the revealing concept of Cognitive Radio (CR) [3]. CR can be defined as a radio platform that is able to adjust its operating parameters in real-time, based on varying requirements and environment's conditions through a process of cognition. Typically, a CR-based system consists of two types of users: the licensed users (Primary Users, PUs) and the unlicensed users (Secondary or Cognitive Users, SUs). PUs can communicate being unaware of SUs' presence, while SUs use the wireless spectrum in a more intelligent and flexible way, without interrupting PUs' communication [4,5]. More specifically, the opportunistic spectrum access of SUs can exploit the unused licensed in-band segments without causing interference to the active PUs. This allocation of the licensed spectrum can be accomplished through overlay or underlay techniques. In spectrum overlay techniques, the SUs are not allowed to transmit their data with the presence of PUs. On the other hand, the spectrum underlay techniques allow the SUs to transmit simultaneously with the PUs as long as they do not affect their communication. Any of these techniques can be used in cognitive radio network design having corresponding advantages and disadvantages.

In this paper, we consider a spectrum underlay CR system that suffers from fading. We analyze the communication quality both from SU's and PU's perspective and we propose a power allocation scheme so as to maximize SU's throughput for specific quality of service (QoS) requirements. Since different services demand different QoS constraints [6,7], the wireless users are expected to tolerate different levels of delay for each service. Thus, especially for real time applications, it is important to take into consideration the impact of the QoS provisioning metric in the system's analysis. A suitable tool that can integrate the rate performance of a wireless link and the key metric of delay QoS requirements is the effective capacity that has recently started to draw the attention of researchers [8,9]. Therefore, in the proposed work we focus on the maximization of SU's effective capacity, while guaranteeing the communication quality of PU's link. Specifically, in order to preserve PU's communication, we employ two types of constraints. The first one refers to the traditional underlay systems' technique, which restricts the transmission power of the SU in order to maintain the interference at primary receiver below a specific value. Regarding the other constraint, we propose the novel limitation of the inverse signal to interference plus noise ratio (SINR) at PU's receiver. This metric is significant for the performance of the PU as apart from the interference power from the SU, it considers the PU's channel variations and also their relative behavior. Moreover, in our analysis we consider the long-term (average) as well as the short-term (peak) nature of these constraints [10]. Consequently, depending on the type and the nature of the interference constraint imposed to the SU, we describe four different scenarios and we find the optimal power allocation and the corresponding effective capacity for each scenario. Assuming perfect channel state information (CSI) of all links, we also include in our analysis the significant impact of PU's interference to SU's link quality [11].

Apart from the above considerations, the novelty of this work is additionally based on the fact that PU's channel variations can be used beneficially for improving the effective capacity of the SU in terms of opportunistically exploiting bad PU's channel conditions that lead to outage events. Particularly, in the proposed work, it is considered that the SU can transmit with its maximum power when the PU experiences an outage event and with the

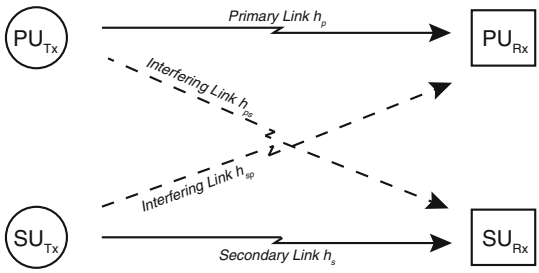

Fig. 1 Cognitive radio system under consideration

optimal power, otherwise. Finally, numerical calculations, validated with simulation results, evaluate the theoretical analysis for various system parameters (QoS requirements, values of constraints and channels characteristics) and the different scenarios are compared both from PU's and SU's side. The expected system behavior is verified and the necessity of the QoS factor is proven.

The rest of the paper is organized as follows. Section 2, presents the system model under consideration and the concept of effective capacity, while Sect. 3 describes briefly previous work in the same research area and highlights our contribution points. In Sect. 4, we analyze the QoS-driven power allocation problem and we present the constraints that should be satisfied by the SU. The solutions of this problem for all the different scenarios are analyzed in Sect. 5 where the expression for the SU's optimal transmission power and the corresponding effective capacity for each scenario are presented. In Sect. 6, we study the impact of the different interference costraints on the communication of the PU whereas in Sect. 7, we evaluate the proposed scheme through numerical calculations and discuss the results. Finally, Sect. 8 concludes the paper.

2 System Model: Effective Capacity

In our system model, a secondary transmitter attempts to send data to a secondary receiver in the presence of a PU. Specifically, as we can see in Fig. 1, a pair of primary transmitter (PU_{Tx}) and receiver (PU_{Rx}) coexists with a pair of secondary transmitter (SU_{Tx}) and receiver (SU_{Rx}). The specific system model is a basic reference model for the theoretical analysis of CR networks [12], which takes into account the interference from/to the PU. However, it should be noted that the proposed mechanism can also be employed in case of a CR network with multiple SUs considering an additional scheduling scheme that allows only to one SU to transmit during each timeslot [13].

In our approach, discrete-time, uncorrelated Nakagami fading channels are considered for the wireless links. The corresponding received signals for the primary and the secondary receiver, at a specific time n, are:

$$y_p[n] = \sqrt{h_p[n]}x_p[n] + \sqrt{h_{sp}[n]}x_s[n] + z_p[n] \quad (1)$$

$$y_s[n] = \sqrt{h_s[n]}x_s[n] + \sqrt{h_{ps}[n]}x_p[n] + z_s[n] \quad (2)$$

where x_p and x_s represent the transmitted signals from the primary and the secondary transmitter respectively, while z_p and z_s represent the additive white Gaussian noise for each corresponding link. Moreover, h_s, h_{sp}, h_p and h_{ps} denote the channel power gains between the secondary/primary transmitter and the secondary/primary receiver, according to Fig. 1.

We must note here that for simplicity reasons, the time index n has been ignored in the rest of the paper.

Due to the fact that the amplitude gains of the fading channels are modeled according to unit-mean Nakagami distribution [14], the probability density function (pdf) of channel power gains is given by the following Gamma distribution:

$$f_{h_j}(h_j) = \frac{m_j^{m_j} h_j^{m_j-1}}{\Gamma(m_j)} e^{-m_j h_j} \tag{3}$$

where $\Gamma(\cdot)$ is the Gamma function [15] and the parameter m_j denotes the ratio of the line of sight (LoS) signal power to that of the multi-path component. More specifically, this parameter models the severity of fading with $m_j = 1$ leading to Rayleigh fading conditions, $m_j = 0.5$ reflecting more severe fading conditions such as one-sided Gaussian fading and $m_j > 1$ resulting in approximations of Rician and lognormal fading channels. Furthermore, we have considered that the noise power spectral density and the system's spectral bandwidth are correspondingly N_0 and B and that data-link layer packets of the secondary link are organized into frames with duration T_f.

In this paper, it is assumed that the primary transmitter is not able to sense the presence of a SU and it transmits with constant power P_p. On the contrary, the secondary nodes are cognitive nodes meaning that they can sense their environment and adapt their power depending on the existence of a PU and the channel conditions. Moreover, we assume that the SU is aware of the CSI of each link. In case of the PU link's and the interference $\mathrm{SU_{Tx}} - \mathrm{PU_{Rx}}$ link, the corresponding channel gains, can be obtained either directly by listening to a feedback from the PU as proposed in [16,17], where there is a collaboration between the PU and SU, or indirectly through a spectrum manager which acts as a referee between the two parts [18,19]. Hence, when a PU transmits data, the SU restricts its transmission power under a specific limit in order not to affect the primary link.

In order to be able to analyze the resource allocation problem, we define the signal-to-noise ratio (SNR) and the SINR for the primary and the secondary receiver as follows:

$$\text{Primary Receiver's SNR :} \quad SNR_p = \frac{h_p \cdot P_p}{N_0 B},$$

$$\text{Primary Receiver's SINR:} \quad SINR_p = \frac{h_p \cdot P_p}{h_{sp} \cdot P_s + N_0 B},$$

$$\text{Secondary Receiver's SINR:} \quad SINR_s = \frac{h_s \cdot P_s}{h_{ps} \cdot P_p + N_0 B}.$$

In general, it is considered that the PU experiences an outage event when its SINR falls below a certain threshold. However, in our theoretical analysis, when we refer that the PU is in outage, we consider the scenario in which the SNR of the PU falls below that threshold and the interfering power is not taken into account.

In order to guarantee that the communication quality of the PU will not be downgraded, we force the SU to limit its transmission power to the adequate level. Depending on the interference constraint imposed to the SU, we study four different scenarios for the power allocation problem. In the first two scenarios, the resource management problem of the SU subject to an average/peak interference power constraint is analyzed whereas in the following two scenarios, we propose a novel interference constraint based on the average/peak inverse SINR of the PU.

The goal of our work is to maximize the throughput of the secondary link considering that the SU should meet specific QoS requirements without however affecting the communication

of the primary link. In order to be able to study the maximum throughput for specific QoS constraints, we employ the concept of effective capacity. The specific concept has been introduced by Wu and Negi [8] as the dual concept of effective bandwidth [20], which represents the minimum constant transmission rate so as to satisfy a certain QoS requirement. Accordingly, the effective capacity function $E_c(\theta)$ refers to the maximum constant arrival rate that the channel can sustain in order to guarantee a QoS requirement denoted by the parameter θ known as the QoS exponent. More specifically, if $\{R[i], i = 1, 2, \ldots\}$ is an uncorrelated discrete-time stationary and ergodic stochastic service process, then the formal definition of the effective capacity is given by:

$$E_c(\theta) = -\frac{1}{\theta} \ln \left(\mathrm{E} \left[e^{-\theta R[i]} \right] \right). \tag{4}$$

The QoS parameter θ is a positive constant that represents the decaying rate of the QoS violation probability. In particular, when the delay bound is the QoS metric of interest, the parameter θ can be defined from the relationship $Pr\{Delay > D_{max}\} \approx e^{-\theta \delta D_{max}}$, where D_{max} denotes the delay bound and δ is jointly determined by both arrival and service processes [8]. It should be noted that a greater θ indicates more strict QoS requirements, whereas smaller values of θ denote more flexible QoS constraints.

3 Related Work and Contributions

Recently, the concept of effective capacity has been employed in order to study resource allocation techniques that incorporate the QoS metric for various terrestrial wireless networks [9,21,22] and satellite networks [23]. However, the research on the analysis of the effective capacity for cognitive radio networks is limited. In [24,25] the authors investigate the effective capacity of the secondary link that can be achieved in Nakagami channels under spectrum sharing constraints assuming an average interference power constraint for the protection of the PU. In [26], the authors study the QoS constrained capacity in Rayleigh fading channels under the peak interference constraint with single and multiple primary receivers. Similarly, Akin and Gursoy [27] study the effective capacity of cognitive radio channels in order to identify the performance of the system in the presence of statistical delay constraints. Specifically, the authors consider that the cognitive radio initially performs channel sensing to detect the activity of PUs and then transmits the data at two different average power levels depending on the presence of active PUs. Finally, in [28], the authors investigate the optimization of effective capacity from SU's perspective in Rayleigh fading environment considering an average interference power constraint so as to protect the communication of the PU. However, in all the referred papers, the authors study the corresponding resource allocation problem, considering either the average or the peak interference power constraint, only from SU's perspective without analyzing each scheme's effect to the primary link communication. Furthermore, they neglect the impact of the PU's interference to the SU which is an important factor in order to design a realistic power allocation scheme.

In this work, our objective is the study of an ameliorated optimal power allocation policy which maximizes the effective capacity of the secondary link under different interference constraints and the comparison of these scenarios both from SU's and PU's perspective. More analytically, the main contributions of our work are the following:

– The proposed power allocation algorithm takes advantage of the channel variations of the primary link. Specifically, in order to optimize the effective capacity of the SU, the

algorithm exploits the time intervals when the PU experiences an outage event due to its own channel state, allowing to the SU to transmit with the maximum power.
– Except from the analysis of the resource allocation problem subject to the traditional interference power constraint, we study the power allocation problem under the proposed novel interference constraint which is based on the inverse SINR of the primary receiver. As it is verified in the numerical analysis section, this constraint allows the SU to exploit the channel variations of the primary link and leads to better results in terms of the SU's effective capacity. Moreover, the use of the specific constraint yields to lower values of PU's outage probability, guaranteing a specific threshold to the communication quality of the primary link.
– In this work, the interference of the primary transmitter to the secondary receiver is taken into account whereas in the literature this factor was ignored. As it is verified in the simulation's section, the impact of the primary transmitter–secondary receiver link is important and should be included in the analysis of the optimal effective capacity in order to design a more realistic power allocation scheme.
– Finally, for both interference constraints (interference power and inverse SINR constraints), we study the outcome of the corresponding optimization problem for short-term (peak) and long-term (average) constraints and we compare each scenario not only from SU's side but also from PU's perspective. We must note that, to the authors' best knowledge, this study consists the first unified analysis in the literature for the optimization of SU's effective capacity that also studies how the quality constraints of the SU affect the PU's communication.

4 Power Allocation Problem

At first, before we proceed to describe the power allocation problem, it's useful to denote the constraints which must be satisfied by the SU.

4.1 Power Constraints of the SU

The first restriction, which is considered in all of the scenarios, refers to a peak power constraint that expresses the device power amplifier's limit (P_{max}) of the secondary transmitter [29]. Specifically, we consider that the peak transmit power of the SU satisfies the following inequality:

$$0 \leq P_s \leq P_{max} \tag{5}$$

Regarding to the impact of the SU's transmission on the PU's communication, we focus on two different types of interference constraints. The first type of constraints is the traditional interference power constraint that represents the received power to the PU from the secondary transmitter. Specifically, we study the case of the average interference power constraint which can be expressed as:

$$E[h_{sp} \cdot P_s] \leq Q_{I,av} \tag{6}$$

and the case of the peak interference power constraint which is the following:

$$h_{sp} \cdot P_s \leq Q_{I,pk} \tag{7}$$

where $Q_{I,av}$ and $Q_{I,pk}$ denote the average and the peak interference power limits at $\mathrm{PU_{Rx}}$, correspondingly.

Concerning the second type of constraints, we propose the use of a significant metric known as the inverse SINR in order to ensure the communication quality of the primary link. Given the fact that the SINR is a good indicator of the performance of a particular link, the inverse SINR (ISINR) can also be employed in order to measure the communication quality of the link [30,31]. Our analysis is separated to the study of the average inverse SINR constraint:

$$E\left[\frac{h_{sp}\cdot P_s + N_0\cdot B}{h_p\cdot P_p}\right] \leq Q_{ISINR,av} \tag{8}$$

and the peak inverse SINR constraint:

$$\frac{h_{sp}\cdot P_s + N_0\cdot B}{h_p\cdot P_p} \leq Q_{ISINR,pk} \tag{9}$$

where $Q_{ISINR,av}$ and $Q_{ISINR,pk}$ denote the average and the peak inverse SINR limits at $\mathrm{PU_{Rx}}$, correspondingly.

In both types of restrictions, the average constraints can be used in cases where the PU provides delay-non sensitive services and thus an average limitation can guarantee a long-term quality to the PU link, whereas the peak constraints can be employed when the PU has to satisfy instantaneous quality requirements.

In the next section, we will study the resource allocation problem for all the possible scenarios, which result from the combination of the peak transmit power constraint with the four interference constraints. Specifically, the sets of the considered SU's transmission power, depending on the specific interference constraints' scenarios are the following: $\Omega_1 = \{P_s : (5), (6)\}$, $\Omega_2 = \{P_s : (5), (7)\}$, $\Omega_3 = \{P_s : (5), (8)\}$ and $\Omega_4 = \{P_s : (5), (9)\}$.

4.2 Problem Definition

In our analysis, we employ the normalized effective capacity $E_{c,n}(\theta)$ (bits/s/Hz) which is defined as the effective capacity divided by the term $T_f B$ and is given by:

$$E_{c,n}(\theta) = \frac{E_c(\theta)}{T_f B} = -\frac{1}{\theta T_f B}\ln\left(\mathrm{E}\left[e^{-\theta R}\right]\right) \tag{10}$$

where R represents the channel capacity of the SU's link that can be defined as:

$$R = T_f B\log_2\left(1+\frac{P_s(\theta,h_{sp},h_s,h_{ps},h_p)h_s}{P_p h_{ps}+N_0 B}\right). \tag{11}$$

Here, we note that the unit for the rate R and the effective capacity $E_c(\theta)$ is "bits per frame". In order to simplify the form of equations, we define the term $a_{SU} = a_{SU}(\theta) = \theta T_f B/\ln(2)$ which represents the normalized QoS exponent. Thus, the normalized effective capacity can be expressed as a function of a_{SU} as follows:

$$E_{c,n}(a_{SU}) = -\frac{1}{a_{SU}\ln(2)}\ln\left(\mathrm{E}\left[\left(1+\frac{P_s(a_{SU},h_{sp},h_s,h_{ps},h_p)h_s}{P_p h_{ps}+N_0 B}\right)^{-a_{SU}}\right]\right). \tag{12}$$

The main goal of our model is to maximize the effective capacity of the secondary link and find the corresponding optimal power control policy of the SU under the restriction not to violate PU's communication. As it will be described, the SU chooses opportunistically its power allocation using CSI at the $\mathrm{SU_{Tx}}$. Moreover, in our work, we consider that the SU exploits the time intervals when the PU is in outage due to its own channel conditions, in

order to increase its achievable effective capacity. This means that when the SNR value of the primary link falls below a certain outage threshold (Q_{out}), the SU transmits with its maximum power. On the other hand, the SU transmits with the optimal power when $SNR_p > Q_{out}$. Thus, the maximization problem can be formulated as follows:

$$E_{c,n}^{*} = \max_{P_s \epsilon \Omega_i} E_{c,n}(a_{SU}) \text{ for } h_p > h_{out} \tag{13}$$

where $i = 1, 2, 3, 4$ denotes the different scenarios and $h_{out} = \frac{Q_{out} \cdot N_0 \cdot B}{P_p}$ denotes the corresponding outage threshold for the PU's channel gain. As it is obvious, in our algorithm, the optimal power allocation is given by $P_s^{*} = P_{max}$ for $h_p \leq h_{out}$.

For simplicity and calculation purposes, we define the following function:

$$g(a_{SU}, P_s(a_{SU}, h_{sp}, h_s, h_{ps}, h_p)) = \mathrm{E}\left[\left(1 + \frac{P_s(a_{SU}, h_{sp}, h_s, h_{ps}, h_p)h_s}{P_p h_{ps} + N_0 B}\right)^{-a_{SU}}\right]. \tag{14}$$

Since $\ln(\cdot)$ is a monotonically increasing function, the maximization problem of the normalized effective capacity can be further reduced to the minimization problem of the auxiliary function $g(a_{SU}, P_s(a_{SU}, h_{sp}, h_s, h_{ps}, h_p))$. In the following section, we present the solutions of the resource allocation problem

$$\min_{P_s \epsilon \Omega_i} \{g(a_{SU}, P_s(a_{SU}, h_{sp}, h_s, h_{ps}, h_p))\} \text{ for } h_p > h_{out} \tag{15}$$

for each of the above described scenarios.

5 Optimal Power Allocation Schemes

5.1 Interference Power Constraint (Scenario A)

In the first two scenarios, we employ the interference power constraint in order to regulate the SU's transmission and guarantee the PU's communication. More specifically, at first, we study the case of the average interference power constraint whereas in the second part, we analyze the case of the corresponding peak constraint.

5.1.1 Average Constraint (Scenario A1)

The first scenario refers to the maximization of the normalized effective capacity subject to the peak SU's transmit power and the average interference power constraints. Specifically, we solve the optimization problem defined in (15) for $P_s \epsilon \Omega_1$. It is proven that the optimal strategy of the SU for the specific scenario is given by:

$$P_s^{*}(a_{SU}, h_{sp}, h_s, h_{ps}, h_p) = \begin{cases} P_{\max} \text{ for } \{h_p \leq h_{out}\} \text{or} \{h_p > h_{out} \text{ and } h_{sp} \leq h_0^A(h_s, h_{ps})\} \\ P_{opt}^A(a_{SU}, h_{sp}, h_s, h_{ps}), \text{ for } h_p > h_{out} \text{ and } h_0^A(h_s, h_{ps}) < h_{sp} \leq h_1^A(h_s, h_{ps}) \\ 0 \ , \quad \text{for } h_p > h_{out} \text{ and } h_{sp} > h_1^A(h_s, h_{ps}) \end{cases} \tag{16}$$

where

$$P_{opt}^{A}(a_{SU}, h_{sp}, h_s, h_{ps}) = \left(\frac{P_p h_{ps} + N_0 B}{h_s}\right)\left\{\left[\frac{\lambda_0 h_{sp}(P_p h_{ps} + N_0 B)}{a_{SU} h_s}\right]^{-\frac{1}{1+a_{SU}}} - 1\right\},$$

$$h_0^A(h_s, h_{ps}) = \frac{a_{SU} h_s}{\lambda_0 (P_p h_{ps} + N_0 B)}\left[\frac{P_{\max} h_s}{P_p h_{ps} + N_0 B} + 1\right]^{-(a_{SU}+1)} \text{ and } h_1^A(h_s, h_{ps})$$
$$= \frac{a_{SU} h_s}{\lambda_0 (P_p h_{ps} + N_0 B)}.$$

The proof of the second branch of Eq. (16) and the computation of the Lagrange multiplier λ_0 from the average interference power constraint is provided in the "Appendix". Using (16), we derive the effective capacity for the optimal power allocation as follows:

$$E_{c,n}^{*}(a_{SU}) = -\frac{1}{a_{SU}\ln(2)}\ln\left\{\left(1 - \frac{\Gamma(m_p, m_p h_{out})}{\Gamma(m_p)}\right)\cdot\int_0^{\infty}(1 + P_{max}x)^{-a_{SU}} f_x(x)dx\right.$$
$$+ \frac{\Gamma(m_p, m_p h_{out})}{\Gamma(m_p)}\cdot\left[\int_0^{\infty}\left(1 - \frac{\Gamma\left(m_{sp}, m_{sp}\lambda_0^{-1} a_{SU} x\,(P_{max}x+1)^{-a_{SU}-1}\right)}{\Gamma(m_{sp})}\right)\right.$$
$$\times (1 + P_{max}x)^{-a_{SU}} f_x(x)dx + \frac{1}{\Gamma(m_{sp})}\cdot\left(\frac{a_{SU} m_{sp}}{\lambda_0}\right)^{-\frac{a_{SU}}{a_{SU}+1}}\int_0^{\infty} x^{-\frac{a_{SU}}{a_{SU}+1}}$$
$$\times\left(\Gamma\left(m_{sp} + \frac{a_{SU}}{a_{SU}+1}, m_{sp}\lambda_0^{-1} a_{SU} x(1 + P_{max}x)^{-a_{SU}-1}\right)\right.$$
$$\left.\left.\left.- \Gamma\left(m_{sp} + \frac{a_{SU}}{a_{SU}+1}, m_{sp}\lambda_0^{-1} a_{SU} x\right)\right) f_x(x)dx\right.\right.$$
$$\left.\left. + \frac{1}{\Gamma(m_{sp})}\int_0^{\infty}\Gamma\left(m_{sp}, m_{sp}\lambda_0^{-1} a_{SU} x\right) f_x(x)dx\right]\right\} \tag{17}$$

where the function $f_x(x)$ is defined in the "Appendix" [see (34)].

5.1.2 Peak Constraint (Scenario A2)

The second scenario refers to the maximization of the normalized effective capacity subject to the peak SU's transmit power and the peak interference power constraint. Thus, we find the solution of the optimization problem defined in (15) for $P_s \epsilon \Omega_2$. From the combination of the two peak constraints of this problem, we can easily conclude to: $P_s(h_{sp}) \leq \min\left\{P_{max}, \frac{Q_{I,pk}}{h_{sp}}\right\}$. Therefore, the optimal power policy of the SU for this scenario can be expressed as:

$$P_s^{*}(h_{sp}, h_p) = \begin{cases} P_{\max}, & \text{for } \{h_p \leq h_{out}\} \text{ or } \{h_p > h_{out} \text{ and } h_{sp} \leq \frac{Q_{I,pk}}{P_{max}}\} \\ \frac{Q_{I,pk}}{h_{sp}}, & \text{for } h_p > h_{out} \text{ and } h_{sp} > \frac{Q_{I,pk}}{P_{max}} \end{cases} \tag{18}$$

Using (18) and (34), the corresponding effective capacity is given by:

$$E^{*}_{c,n}(a_{SU}) = -\frac{1}{a_{SU}\ln(2)}\ln\left\{\left(1-\frac{\Gamma(m_p, m_p h_{out})}{\Gamma(m_p)}\right)\cdot\int_0^{\infty}(1+P_{max}x)^{-a_{SU}}\, f_x(x)dx\right.$$
$$+\frac{\Gamma(m_p, m_p h_{out})}{\Gamma(m_p)}\cdot\left[\left(1-\frac{\Gamma\left(m_{sp}, m_{sp}Q_{I,pk}/P_{max}\right)}{\Gamma(m_{sp})}\right)\cdot\int_0^{\infty}(1+P_{max}x)^{-a_{SU}}\, f_x(x)dx\right.$$
$$\left.\left.+\int_{\frac{Q_{I,pk}}{P_{max}}}^{\infty}\int_0^{\infty}\left(1+\frac{Q_{I,pk}x}{h_{sp}}\right)^{-a_{SU}}\cdot f_x(x)\, f_{h_{sp}}(h_{sp})dx\,dh_{sp}\right]\right\}. \tag{19}$$

From (16)–(19), we can observe that in the specific type of interference constraint (Scenario A), the SU doesn't need to be aware of the instantaneous channel conditions of the PU but only of the time intervals when the primary link falls in outage. In the numerical results section, Scenarios A1 and A2 are compared in terms of the achieved effective capacity and their corresponding power allocation policy.

5.2 Inverse SINR Constraint (Scenario B)

In this subsection, we employ the novel constraint based on the concept of the inverse SINR in order to limit the interference from the SU_{Tx} to the PU_{Rx}. At first, we present the solution of the optimization problem with the average inverse SINR constraint whereas the second part includes the solution of the resource allocation problem under the corresponding peak constraint.

5.2.1 Average Constraint (Scenario B1)

The specific scheme refers to the maximization of the effective capacity subject to the peak transmit power and the average inverse SINR constraint. Thus, we study the optimization problem in (15) where $P_s \epsilon \Omega_3$ and we find the optimal strategy for the SU which is defined by:

$$P_s^{*}(a_{SU}, h_{sp}, h_s, h_{ps}, h_p) = \begin{cases} P_{\max}, & \text{for } \{h_p \le h_{out}\} \text{ or } \{h_p > h_{out} \text{ and } h_{sp} \le h_0^B(h_s, h_{ps}, h_p)\} \\ P^B_{opt}(a_{SU}, h_{sp}, h_s, h_{ps}, h_p), & \text{for } h_p > h_{out} \text{ and } h_0^B(h_s, h_{ps}, h_p) < h_{sp} \le h_1^B(h_s, h_{ps}, h_p) \\ 0, & \text{for } h_p > h_{out} \text{ and } h_{sp} > h_1^B(h_s, h_{ps}, h_p) \end{cases} \tag{20}$$

where

$$P^B_{opt}(a_{SU}, h_{sp}, h_s, h_{ps}, h_p) = \left(\frac{P_p h_{ps} + N_0 B}{h_s}\right)\left\{\left[\frac{\lambda_0' h_{sp}(P_p h_{ps} + N_0 B)}{a_{SU} h_s P_p h_p}\right]^{-\frac{1}{1+a_{SU}}} - 1\right\},$$
$$h_0^B(h_s, h_{ps}, h_p) = h_0^A(h_s, h_{ps}) h_p P_p \quad \text{and} \quad h_1^B(h_s, h_{ps}, h_p) = h_1^A(h_s, h_{ps}) h_p P_p.$$

For brevity reasons, we omit the proof of (20) which is similar to that of Scenario A1. Moreover, the value of the Lagrange multiplier λ_0' can be found from the satisfaction of the average inverse SINR constraint. Using (20) and (34), the effective capacity for the optimal power allocation is obtained as follows:

$$
\begin{aligned}
E_{c,n}^{*}(a_{SU}) = &-\frac{1}{a_{SU}\ln(2)}\ln\Bigg\{\left(1-\frac{\Gamma(m_p, m_p h_{out})}{\Gamma(m_p)}\right)\cdot\int_0^{\infty}(1+P_{max}x)^{-a_{SU}}\, f_x(x)dx \\
&+\int_{h_{out}}^{\infty}\int_0^{\infty}(1+P_{max}x)^{-a_{SU}}\left(1-\frac{\Gamma\left(m_{sp}, m_{sp}(\lambda_0')^{-1}a_{SU}xP_ph_p\,(P_{max}x+1)^{-a_{SU}-1}\right)}{\Gamma(m_{sp})}\right) \\
&\times f_{h_p}(h_p)f_x(x)dxdh_p + \frac{1}{\Gamma(m_{sp})}\cdot\int_{h_{out}}^{\infty}\int_0^{\infty}\left(\frac{xa_{SU}P_ph_pm_{sp}}{\lambda_0'}\right)^{\frac{-a_{SU}}{a_{SU}+1}} \\
&\cdot\Bigg[\Gamma\left(m_{sp}+\frac{a_{SU}}{a_{SU}+1}, m_{sp}(\lambda_0')^{-1}a_{SU}xP_ph_p(P_{max}x+1)^{-a_{SU}-1}\right) \\
&-\Gamma\left(m_{sp}+\frac{a_{SU}}{a_{SU}+1}, m_{sp}(\lambda_0')^{-1}a_{SU}xP_ph_p\right)\Bigg]\cdot f_{h_p}(h_p)f_x(x)dxdh_p + \frac{1}{\Gamma(m_{sp})} \\
&\cdot\int_{h_{out}}^{\infty}\int_0^{\infty}\Gamma\left(m_{sp}, m_{sp}(\lambda_0')^{-1}a_{SU}xP_ph_p\right)f_{h_p}(h_p)f_x(x)dxdh_p\Bigg\}. \qquad (21)
\end{aligned}
$$

5.2.2 Peak Constraint (Scenario B2)

The last scenario refers to the maximization of the effective capacity subject to the peak SU's transmit power and the peak inverse SINR constraint. Here, we solve the optimization problem in (15) where $P_s \epsilon \Omega_4$. The solution can be easily found from the combination of the two peak constraints. Thus, it can be proven that the optimal policy of the SU is the following:

$$
P_s^{*}(h_{sp}, h_p) = \begin{cases} P_{\max}, & \text{for } \{h_p \le h_{out}\} \text{ or } \{h_p > h_{qual} \text{ and } h_{sp} \le h_0^C(h_p)\} \\ \frac{Q_{ISINR,pk}h_pP_p - N_0B}{h_{sp}}, & \text{for } h_p > h_{qual} \text{ and } h_{sp} > h_0^C(h_p) \\ 0, & \text{for } h_{out} < h_p \le h_{qual} \end{cases} \qquad (22)
$$

where

$$
h_{qual} = \frac{N_0B}{Q_{ISINR,pk}P_p} \text{ and } h_0^C(h_p) = \frac{Q_{ISINR,pk}h_pP_p - N_0B}{P_{max}}.
$$

Correspondingly, the effective capacity for the optimal power allocation can be expressed as:

$$E_{c,n}^{*}(a_{SU}) = -\frac{1}{a_{SU}\ln(2)}\ln\Bigg\{\Bigg(1-\frac{\Gamma(m_p, m_p h_{out})}{\Gamma(m_p)}\Bigg)\cdot\int_0^{\infty}(1+P_{max}x)^{-a_{SU}}\ f_x(x)dx$$
$$+\int_{h_{qual}}^{\infty}\int_0^{\infty}(1+P_{max}x)^{-a_{SU}}\cdot\Bigg(1-\frac{\Gamma\left(m_{sp}, m_{sp}(P_{max})^{-1}(Q_{ISINR,pk}h_p P_p - N_0 B)\right)}{\Gamma(m_{sp})}\Bigg)$$
$$\cdot f_{h_p}(h_p)\ f_x(x)\ dxdh_p\ +\ \frac{\left(\Gamma(m_p, m_p h_{out}) - \Gamma(m_p, m_p h_{qual})\right)}{\Gamma(m_p)}$$
$$+\int_{h_0^C}^{\infty}\int_{h_{qual}}^{\infty}\int_0^{\infty}\Bigg(1+\frac{x(Q_{ISINR,pk}h_p P_p - N_0 B)}{h_{sp}}\Bigg)^{-a_{SU}}$$
$$\times f_{h_{sp}}(h_{sp}) f_{h_p}(h_p) f_x(x)dx\ dh_p dh_{sp}\Bigg\}. \tag{23}$$

6 Effect of Interference Constraints on PU's Communication

In this section, we study the impact of the different interference constraints and the corresponding SU's optimal power transmission schemes on the PU's communication. In order to evaluate which constraint (average or peak) leads to better results for the PU, we compare its effective capacity for both the scenarios. As it has been considered above, the PU employs constant power allocation with transmission power P_p. In the following comparative analysis on the achieved values of PU's effective capacity under the interference constraints, we consider obviously the time period that PU is not in outage due to its own channel conditions. That means that we refer to the effective capacity of the PU for values of the primary link's channel power gain greater from the outage threshold (h_{out}) since for lower values the SU transmits with the same power (P_{max}) independently of the nature of the constraint.

6.1 Interference Power Constraint

For fair comparison, we have considered the same average and peak threshold values ($Q_{I,pk} = Q_{I,av} = Q$). Considering that the PU transmits with power equal to P_p, its normalized effective capacity is given by the following equation.

$$E_{c,n,PU} = -\frac{1}{a_{PU}\ln(2)}\ln\Bigg(\mathrm{E}\Bigg[\Bigg(1+\frac{h_p P_p}{h_{sp}P_s(a_{SU}, h_{sp}, h_s, h_{ps}) + N_0 B}\Bigg)^{-a_{PU}}\Bigg]\Bigg) \tag{24}$$

where a_{PU} is the normalized QoS exponent of the PU.

In case of the peak interference constraint, the corresponding effective capacity is expressed as:

$$E_{c,n,PU}^{pk} = -\frac{1}{a_{PU}\ln(2)}\ln\Bigg(\mathrm{E}_{\mathrm{h_p}}\Bigg[\Bigg(1+\frac{h_p P_p}{Q + N_0 B}\Bigg)^{-a_{PU}}\Bigg]\Bigg) \tag{25}$$

where $\mathrm{E_x}(f(x))$ denotes the expected value of $f(x)$ with respect to the random variable x. Regarding the the effective capacity under the average interference constraint, we have

$$\begin{aligned} E_{c,n,PU}^{av} &= -\frac{1}{a_{PU}\ln(2)}\ln\left(\mathrm{E}_{\mathrm{h_p},\mathrm{h_{sp}},\mathrm{h_s},\mathrm{h_{ps}}}\left[\left(1+\frac{h_pP_p}{h_{sp}P_s+N_0B}\right)^{-a_{PU}}\right]\right) \\ &\overset{a_{PU}<1}{\geq} -\frac{1}{a_{PU}\ln(2)}\ln\left(\mathrm{E}_{\mathrm{h_p}}\left[\left(1+\frac{h_pP_p}{\mathrm{E}_{\mathrm{h_{sp}},\mathrm{h_s},\mathrm{h_{ps}}}\left[h_{sp}P_s\right]+N_0B}\right)^{-a_{PU}}\right]\right) \\ &= -\frac{1}{a_{PU}\ln(2)}\ln\left(\mathrm{E}_{\mathrm{h_p}}\left[\left(1+\frac{h_pP_p}{Q+N_0B}\right)^{-a_{PU}}\right]\right) \\ &= E_{c,n,PU}^{pk} \end{aligned} \tag{26}$$

The inequality in the (26) is proven as follows: Defining the function $f(x) = \left(1+\frac{h_pP_p}{x+N_0B}\right)^{-a_{PU}}$ and taking the second derivative of this function, it is easy to prove that its convexity depends on the value of the parameter a_{PU}. More specifically, when $a_{PU} < 1$, $f(x)$ is strictly concave. Combining Jensen inequality [32] and the fact that $f(x)$ is concave for these values of a_{PU}, the inequality $\mathrm{E}[f(x)] \leq f(\mathrm{E[x]})$ holds and consequently, the above expression (26) has been proven. Thus, when the PU has looser QoS constraints ($a_{PU} < 1$), the average interference constraint leads to better effective capacity. However, the opposite is true when there are stricter quality constraints to the PU as it can be verified in the simulations section.

6.2 Inverse SINR Constraint

In this case, we have also considered the same average and peak threshold values ($Q_{ISINR,pk} = Q_{ISINR,av} = Q$). The effective capacity, in case of the peak ISINR constraint, can be expressed as:

$$E_{c,n,PU}^{pk} = -\frac{1}{a_{PU}\ln(2)}\ln\left[\left(1+\frac{1}{Q}\right)^{-a_{PU}}\right] \tag{27}$$

Therefore,

$$\begin{aligned} E_{c,n,PU}^{av} &= -\frac{1}{a_{PU}\ln(2)}\ln\left(\mathrm{E}_{\mathrm{h_p},\mathrm{h_{sp}},\mathrm{h_s},\mathrm{h_{ps}}}\left[\left(1+\frac{h_pP_p}{h_{sp}P_s+N_0B}\right)^{-a_{PU}}\right]\right) \\ &\overset{a_{PU}<1}{\geq} -\frac{1}{a_{PU}\ln(2)}\ln\left[\left(1+\frac{1}{Q}\right)^{-a_{PU}}\right] \\ &= E_{c,n,PU}^{pk} \end{aligned} \tag{28}$$

Similarly to (26), it can be proven that the inequality in (28) holds also for $a_{PU} < 1$. Conclusively, the superiority in terms of PUs effective capacity of the average/peak constraints depends on PUs quality requirements.

7 Numerical Results and Discussion

In order to study the outcome of the resource allocation policy both from SU's and PU's perspective, we separate this section in two parts. In the first part, we present numerical

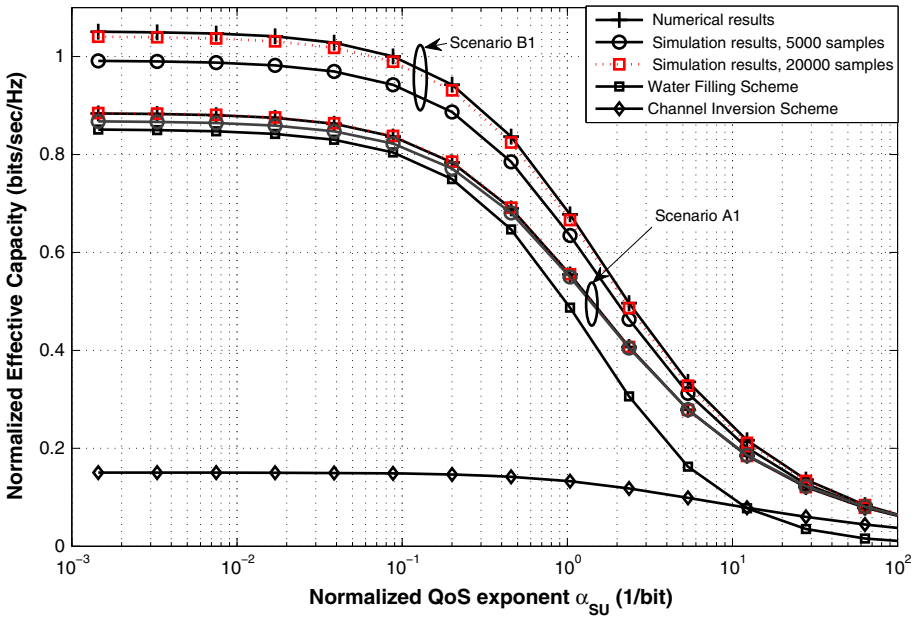

Fig. 2 Normalized effective capacity versus the normalized QoS exponenent α_{SU}: verification of numerical results and comparison of the proposed scheme with reference power allocation techniques

results regarding the optimal power allocation and the corresponding effective capacity of the SU for each of the above scenarios whereas in the second part, we focus on the impact of these constraints on the PU's communication quality. Moreover, at this point, we have to note that the numerical calculations have been validated with extended simulation results.

Without loss of generality, we consider $N_0 B = 10^{-2}\,\mathrm{W}$ and $T_f B = 1$. Also, we have assumed that the transmission power limit of the SU is equal to $P_{max} = P_p = 1\,\mathrm{W}$, the SNR outage threshold of PU is $Q_{out} = 5\,\mathrm{dB}$ and the inverse SINR limits to the $\mathrm{PU_{R_x}}$ are $Q_{ISINR,av} = Q_{ISINR,pk} = -5\,\mathrm{dB}$ unless it is otherwise stated. We must note that the values of the interference power constraints ($Q_{I,av} = Q_{I,pk}$) in Scenario A have been computed so as to lead to the same average inverse SINR of the PU compared to Scenario B. Moreover, the values of the Nakagami parameters are considered as $m_{sp} = m_s = m_{ps} = 1$ whereas $m_p = 1.5$ except from Figs. 2, 3, 4 and 5 in which different values are referred.

7.1 SU's Perspective

At first, Fig. 2 presents the secondary link's normalized effective capacity using the proposed scheme, as it is computed though numerical calculations and Monte–Carlo simulations in order to verify the accuracy of the computations. Furthermore, for comparison purposes, this figure also presents the SU's normalized effective capacity using two reference power allocation schemes. In this case, we have considered that the Nakagami parameters are equal for all the links ($m_{sp} = m_s = m_{ps} = m_p = 1$). It should be noted that due to limited space, for the comparison of numerical and simulation results, we have considered only the cases of average constraints' scenarios (Scenario A1 and B1). As it can be seen from Fig. 2,

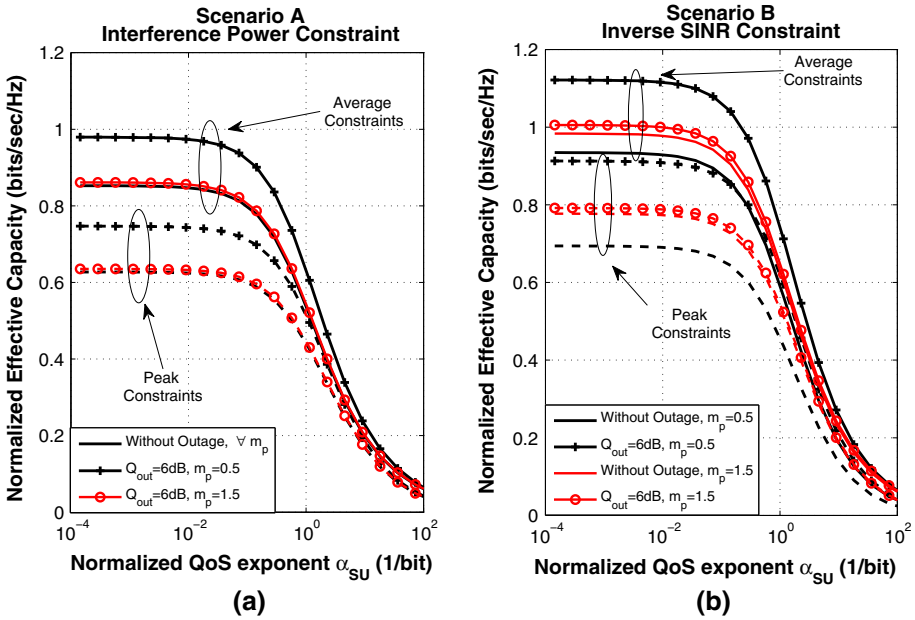

Fig. 3 Normalized effective capacity versus the normalized QoS exponent a for different power allocation techniques and different values of m_p. The *solid curves* represent the average constraints' scenario whereas the *dashed curves* refer to the peak constraints' scenario

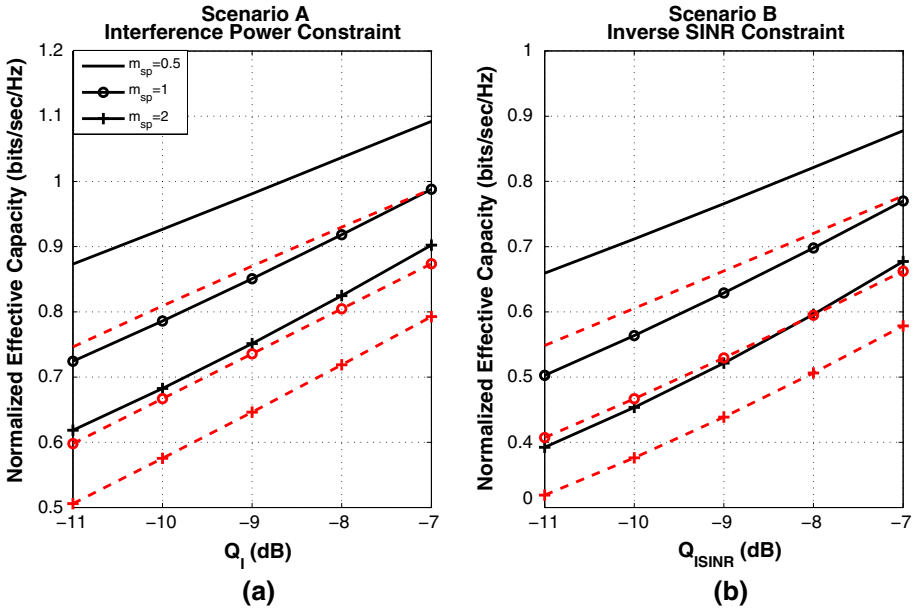

Fig. 4 Normalized effective capacity versus the interference limit for different values of m_{sp}. The *solid curves* represent the average constraints' scenario whereas the *dashed curves* refer to the peak constraints' scenario

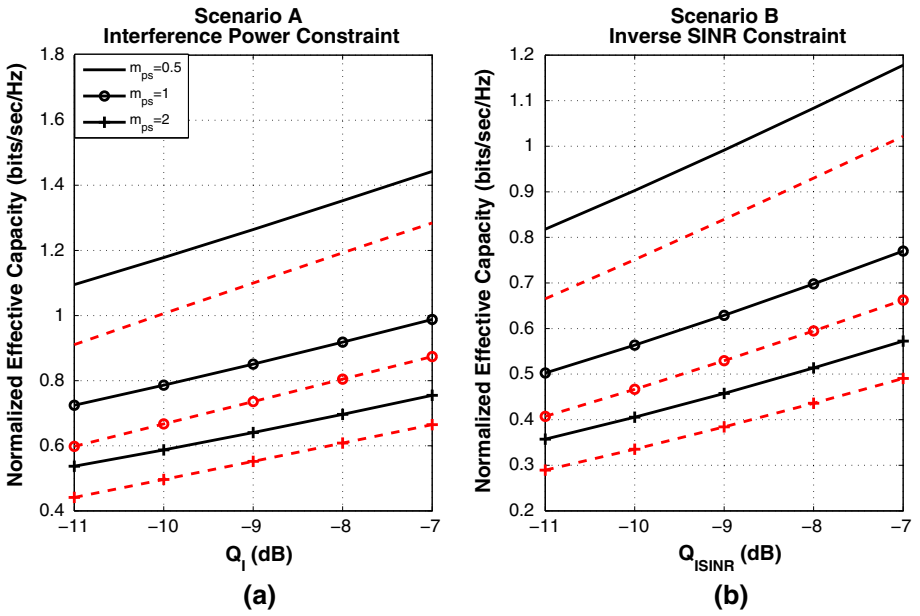

Fig. 5 Normalized effective capacity versus the interference limit for different values of m_{ps}. The *solid curves* represent the average constraints' scenario whereas the *dashed curves* refer to the peak constraints' scenario

the simulation results for 5×10^3 realizations of Nakagami-m fading channels lead to small deviation of the computed normalized effective capacity compared to the numerical results. However, as the number of realizations increases, the computation of the effective capacity becomes more accurate and the simulation results match very well with the corresponding numerical results.

This figure presents also the comparison of the proposed mechanism with two well-known power allocation schemes. The first scheme refers to the water-filling approach for CR networks which optimizes the SU's ergodic capacity under an average interference constraint [29]. Regarding the second scheme, it refers to the channel inversion mechanism [33], the objective of which is to inverse the channel fading so as to provide a constant rate given the average interference constraint. As it can be seen, the proposed mechanism outperforms significantly the two other schemes for all the values of QoS exponent a_{SU}. More specifically, we can observe that the total channel inversion mechanism leads to worse performance compared to the proposed mechanism even for higher values of parameter a_{SU} where the inversion mechanism outperforms the water-filling scheme. Furthermore, it can be seen that the proposed mechanism is also better than the water-filling approach (even for lower values of QoS exponent a_{SU}) due to the exploitation technique of PUs' outage events.

Figure 3 represents the normalized effective capacity of the secondary link versus the normalized QoS exponent a_{SU}, considering different values of m_p. In order to highlight the benefits from PU's outage events' exploitation, we also compare, in this figure, the proposed power allocation scheme with the corresponding one that does not take advantage of the outage events (similar to the power allocation scheme proposed in [25]). We must note here that in all the figures from Figs. 3, 4, 5 and 6, the solid curves correspond to the scenarios with the average interference constraints, whereas the dashed curves refer to the corresponding peak interference constraint scenarios. Depending on the type of the interference constraint, Fig. 3 consists of two subfigures. More specifically, Fig. 3a refers

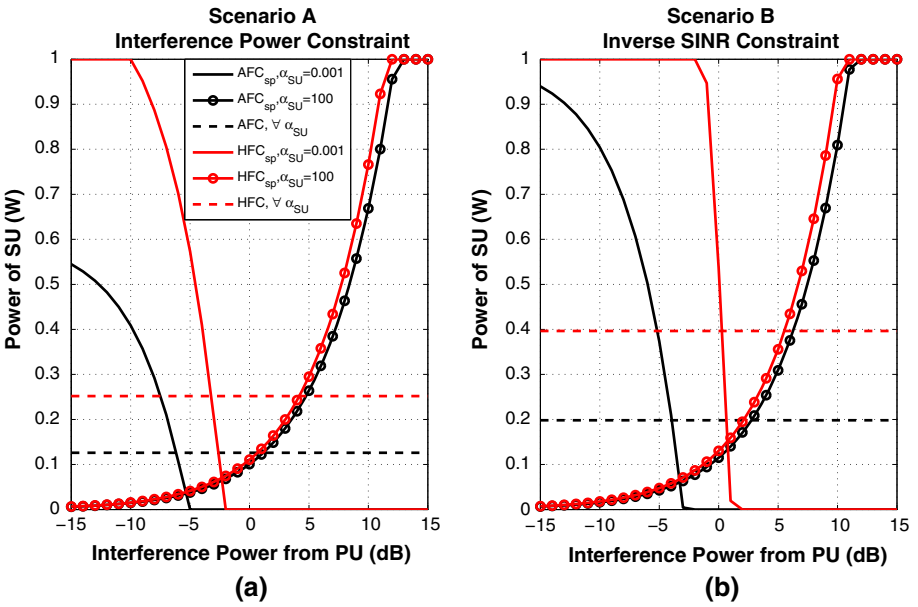

Fig. 6 Optimal power allocation of the SU versus the interference from the PU for different values of the normalized QoS exponent a and for different conditions of the $\mathrm{SU_{Tx}} - \mathrm{PU_{Rx}}$ interference channel. The *solid curves* represent the average constraints' scenario whereas the *dashed curves* refer to the peak constraints' scenario

to the interference power scenarios, whereas Fig. 3b refers to the inverse SINR scenarios. Observing both the subfigures, we can see that the increase of the normalized QoS exponent leads to the decrease of the effective capacity independently of the scenario. This means that when the system has stricter QoS constraints, the SU can achieve low values of effective capacity, whereas when there are looser QoS requirements, the SU can get much higher values of $E_{c,n}$.

Another comment that holds for both the subfigures is that the use of average constraints leads to higher values of effective capacity compared to the corresponding peak constraints. This observation can be justified considering that the average constraints provide more flexibility to the SU allowing him to dynamically allocate its transmission power over different fading states so as to achieve higher $E_{c,n}$. Furthermore, a common remark is that the proposed power allocation technique, which incorporates the maximum power transmission of SU when the PU is in outage, results in an increase of the effective capacity compared to the simple optimal power allocation algorithm that does not use the outage policy. Consequently, it is verified that the SU can benefit from the outage events of the PU ameliorating its throughput for specific QoS requirements.

Regarding the impact of the parameter m_p to the values of the effective capacity, we can observe, that as m_p decreases, the $E_{c,n}$ of the SU increases in the case of the proposed power allocation policy. This can be justified considering that a decrease in m_p means that the primary link experiences more severe fading conditions. Thus, there is a higher probability for the PU to fall into outage due to its own channel characteristics. As the SU takes advantage of the PU's outage events by transmitting at maximum power, lower values of m_p lead basically to higher values of $E_{c,n}$. Regarding the simple power allocation method (without the outage policy), we can see that the change of the value of m_p does not affect at all the effective capacity in the interference power constraint scenarios as the optimal power

allocation doesn't depend on the primary link channel conditions. On the contrary, this is not true for the inverse SINR constraint scenarios where the corresponding simple optimal power allocation depends on the PU's channel characteristics. More specifically, we can observe that in this case, when the primary link does not suffer from severe fading (greater values of m_p), the SU is allowed to transmit at higher power levels and thus increase its $E_{c,n}$.

Finally, comparing the two subfigures in Fig. 3, we can notice that the inverse SINR constraint (Scenario B) leads to better results in terms of SU's effective capacity compared to the corresponding traditional interference power constraint (Scenario A). This outcome can be justified considering that in Scenario B, the SU is more flexible to adapt its power as it depends also on the primary link's channel gain.

In Fig. 4a, b, the normalized effective capacity versus the interference constraint for different values of the $\mathrm{SU_{Tx}} - \mathrm{PU_{Rx}}$ link fading parameter, m_{sp}, is depicted. The first remark here is that for increasing values of the interference constraint, the normalized effective capacity also increases. This can be explained considering that an increase in the interference limit basically means that the SU is allowed to transmit at higher power levels and thus increase its $E_{c,n}$. Moreover, we can observe that the effective capacity increases for lower values of the parameter m_{sp}. This demonstrates that as higher values of m_{sp} correspond to less severe fading conditions of the $\mathrm{SU_{Tx}} - \mathrm{PU_{Rx}}$ interference link, the SU has to transmit at lower power levels in order not to harm the communication of the PU.

Similarly, in Fig. 5, we present the normalized effective capacity versus the interference limit for different values of the $\mathrm{PU_{Tx}} - \mathrm{SU_{Rx}}$ link fading parameter m_{ps}. As we can observe here, the effective capacity decreases for increasing values of the parameter m_{ps}. This can be justified taking into consideration that when the $\mathrm{PU_{Tx}} - \mathrm{SU_{Rx}}$ channel is good (higher values of m_{ps}), the PU interferes much more to the SU's communication. Comparing Figs. 4 and 5, we can see that the impact of the $\mathrm{PU_{Tx}} - \mathrm{SU_{Rx}}$ link is much more significant than the impact of the $\mathrm{SU_{Tx}} - \mathrm{PU_{Rx}}$ link. More specifically, we observe that for a specific interference limit and for the same increase of the Nakagami parameter from $m_{sp} = m_{ps} = 0.5$ to $m_{sp} = m_{ps} = 1$, the decrease of the SU' s effective capacity is almost treble for the case of the m_{ps} parameter compared to the m_{sp} parameter. Consequently, we confirm the fact that the interference from the PU plays an important role to the power allocation of the SU and it should be included in the analysis of the cognitive radio scenario in order to be more realistic.

Figure 6 represents the optimal power allocation of the SU versus the interference power from the PU, for different values of the normalized QoS exponent and for different channel conditions of the $\mathrm{SU_{Tx}} - \mathrm{PU_{Rx}}$ link. The acronyms AFC_{sp} and HFC_{sp} denote average fading conditions and heavy fading conditions of the $\mathrm{SU_{Tx}} - \mathrm{PU_{Rx}}$ link, correspondingly. We consider that in the average fading scenario the channel power gain is equal to its statistical mean whereas in the heavy fading scenario, there is an additional 3 dB loss at channel power gain. Our first remark here is that both the Scenarios A and B have the same behavior regarding the impact of the interference from PU and the QoS exponent. More specifically, regarding the average constraints' scenarios (solid curves), we can observe that when the system has looser QoS constraints (small values of a_{SU}), the SU transmits at higher power levels when there is not interference from the PU so as to maximize its effective capacity. On the contrary, when the system has strict QoS requirements, the SU has to transmit at higher power levels when there is significant interference from the PU in order to eliminate its impact and guarantee a specific communication quality to the secondary link. As far as it concerns the peak constraints' scenarios (dashed curves), we can observe that the corresponding optimal power allocation is independent both from the PU's interference and the QoS exponent (see (18) and (22)). Another observation is that depending on the channel conditions of the interference $\mathrm{SU_{Tx}} - \mathrm{PU_{Rx}}$ link, the SU is allowed to transmit at different power levels. In

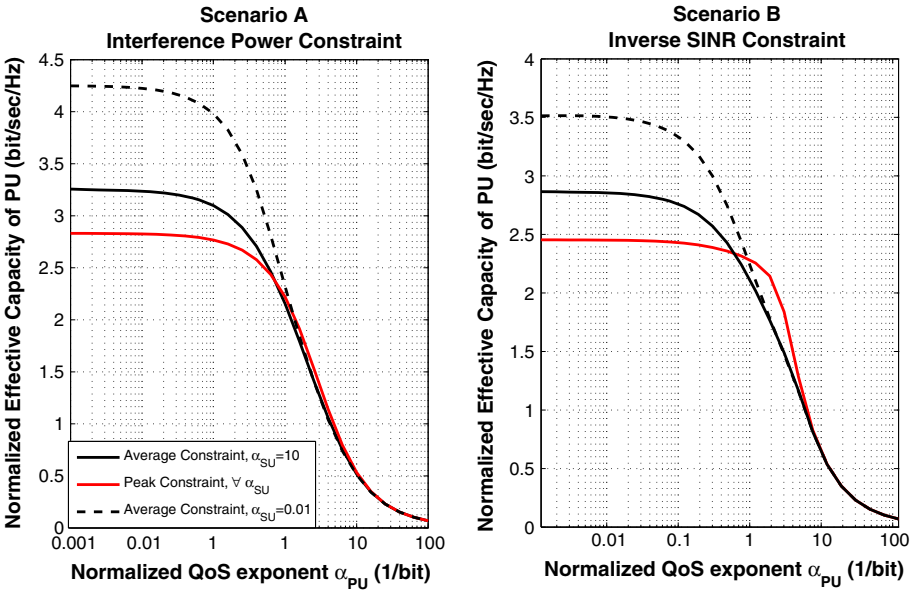

Fig. 7 Normalized effective capacity of PU versus the normalized QoS exponent a_{PU} for different values of SU's QoS exponent (a_{SU})

particular, when the specific channel experiences heavy fading conditions, the SU is allowed to transmit at much higher power levels considering that he will not affect the communication of the PU, due to the advantage of the higher signal's attenuation.

7.2 PU's Perspective

In this subsection, we present the impact of the different interference scenarios on the PU's communication. Figure 7 represents the normalized effective capacity of the PU versus its normalized QoS exponent for different values of the SU's QoS exponent a_{SU}. As it is proven in Sect. 6, we can observe that the average interference constraints lead to better results when the PU has more flexible quality requirements, whereas the peak constraints are more suitable when the PU has strict QoS constraints. Another interesting remark is that for higher values of the SU's QoS exponent, the effective capacity of the PU decreases, under the average constraints. That shows that the quality requirements of the SU influence also the maximum rate that the PU can achieve for specific QoS requirements. On the contrary, as it is expected, the PU's effective capacity for the peak interference scenarios does not depend on the a_{SU}.

Another important metric for the PU's communication is the outage probability. Figure 8 represents the outage probability of the PU for all the different scenarios and for two different values of the SU's normalized QoS exponent a_{SU}. We must note here that in this case, the inverse SINR and the interference power constraints have been considered so as to guarantee a certain level of communication quality to the PU ($Q_{ISINR} = -10$ dB) whereas the outage SINR threshold varies from -5 to 8 dB. The black solid curve with circular markers represents the probability that the PU falls in outage due to its own channel conditions, without taking into consideration the interference from SU. An initial remark is that the peak constraints lead to lower outage probability of the PU compared to the corresponding average constraints, independently of a_{SU}, which is expected considering that the peak nature of constraints is more strict for the SU's power allocation. Moreover, we notice that using the peak inverse

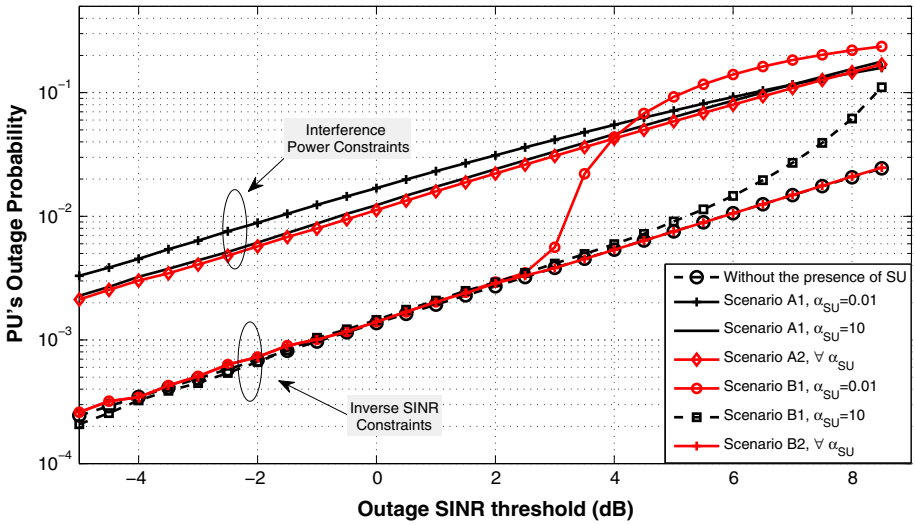

Fig. 8 PU's Outage Probability versus different outage SINR thresholds

SINR constraint, we can ensure that the PU will not experience any outage events due to the presence of the SU. As we can observe in Fig. 8, in case where the SU has looser QoS requirements ($a_{SU} = 0.01$), the inverse SINR constraints lead to significantly smaller values of outage probability compared to the interference power constraints, for lower values of outage threshold. However, for greater values of outage SINR threshold, the opposite is true. On the contrary, if the SU's has stricter QoS constraints ($a_{SU} = 10$), the outage probability of the PU has much lower values for the scenario with the ISINR constraints independently of the value of the outage threshold. The impact of the SU's QoS exponent on the PU's SINR can be justified considering that the average allocated power of the SU changes according to the parameter a_{SU}. More specifically, as we can see in Fig. 9, the SU's average power for the scenarios with the average constraints decreases as the QoS exponent increases. Thus, for greater values of a_{SU}, the interference from the SU to the PU gets lower values, leading also to lower values of outage probability. As it is expected, in case of the peak constraints, the average power of the SU remains stable independently of a_{SU}, which verifies the fact that the outage probability in these cases is not affected by this parameter.

8 Conclusion

In this paper, we have studied an efficient optimal power allocation policy of the SU, in order to maximize its effective capacity, in an underlay cognitive radio network. Considering Nakagami fading conditions for the communication links, the proposed policy takes into account the QoS provisioning metric of SU, while on the same time it guarantees the communication quality of the PU's link through four different interference constraint scenarios: the traditional peak/average interference power constraint and the novel peak/average inverse SINR constraint. Moreover, the proposed power allocation scheme improves the SU's effective capacity including an additional policy that exploits the PU's outage events. In order to study the proposed power allocation also from PU's perspective, we present the impact of different constraints on the PU's communication. Numerical calculations evaluate the performance of

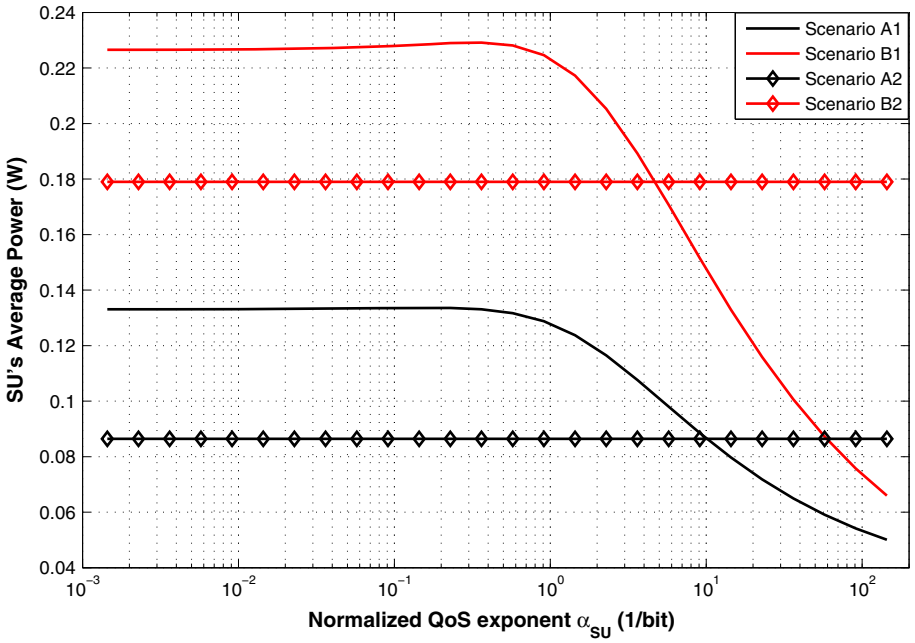

Fig. 9 SU's Average Power versus normalized QoS exponent α_{SU}

the proposed scheme for the different scenarios and confirm that the outage policy actually improves significantly the SU's effective capacity and that the interference caused by the PU to the SU's communication plays a major role in order to study a more realistic analysis. Moreover, comparing the different schemes in terms of SU's effective capacity, we conclude that the average constraints lead to better results than the peak constraints and also that the inverse SINR constraints outperform the interference power constraints. From the PU's perspective, the peak constraints yield to better results in terms of effective capacity when the PU has strict QoS requirements whereas the opposite is true for looser quality constraints. Also, in most cases, the inverse SINR constraints result in lower outage probability of the PU compared to the interference power constraints.

Acknowledgments This work was supported by the Operational Program "Education and Lifelong Learning" under the project ARISTEIA II - FLAME, GSRT No. 3770, in National Technical University of Athens.

Appendix

The solution of (15) for $P_s \epsilon \Omega_1$ can be found by using the Lagrange function that is defined as:

$$L = \int_{h_{out}}^{\infty}\int_{0}^{\infty}\int_{0}^{\infty}\int_{0}^{\infty}\left(1+\frac{P_s(a_{SU},h_{sp},h_s,h_{ps},h_p)h_s}{P_p h_{ps}+N_0 B}\right)^{-a_{SU}} f_{ch}(h_s,h_{ps},h_{sp},h_p)dh_s dh_{ps}dh_{sp}dh_p$$
$$+\lambda_0\left\{\int_{h_{out}}^{\infty}\int_{0}^{\infty}\int_{0}^{\infty}\int_{0}^{\infty} h_{sp}P_s(a_{SU},h_{sp},h_s,h_{ps},h_p)f_{ch}(h_s,h_{ps},h_{sp},h_p)dh_s dh_{ps}dh_{sp}dh_p - Q_{I,av}\right\} \quad (29)$$

where $f_{ch}(h_s, h_{ps}, h_{sp}, h_p) = f_{h_s}(h_s) f_{h_{ps}}(h_{ps}) f_{h_{sp}}(h_{sp}) f_{h_p}(h_p)$ denotes the joint *pdf* of the uncorrelated fading channel power gains. Giving the fact that the optimal solution should satisfy the Lagrange–Euler equation [34,35] we get the following equation:

$$-\frac{a_{SU} h_s}{P_p h_{ps} + N_0 B}\left(1 + \frac{P_s(a_{SU}, h_{sp}, h_s, h_{ps}, h_p) h_s}{P_p h_{ps} + N_0 B}\right)^{-a_{SU}-1} + \lambda_0 h_{sp} = 0 \tag{30}$$

Solving the above with respect to P_s, we found the optimal power allocation defined in (16). The value of the parameter λ_0 can be found from the satisfaction of the average interference power constraint:

$$\int_{h_{out}}^{\infty}\int_{0}^{\infty}\int_{0}^{\infty}\int_{0}^{\infty} h_{sp} \cdot P_s^*(h_s, h_{sp}, h_{ps}, h_p) \cdot f_{ch}(h_s, h_{ps}, h_{sp}, h_p) dh_s dh_{sp} dh_{ps} dh_p = Q_{I,av} \tag{31}$$

In the following, we simplify the integration part by finding the *pdf* of the random variable $\frac{h_s}{h_{ps} P_p + N_0 B}$ where h_s and h_{ps} follow the Gamma distribution with parameters m_s and m_{ps}, respectively. In order to do that, at first we define two new random variables $g_0 = h_{ps} P_p + N_0 B$ and $g_1 = h_s$. Taking into account that $dh_s dh_{ps} = \frac{1}{P_p} dg_0 dg_1$, the joint *pdf* $f_{h_s,h_{ps}}(h_s, h_{ps})$ of the uncorrelated channel power gains can be easily transformed to $f_{g_0,g_1}(g_0, g_1)$ with the simple substitution of the variables.

Afterwards, we define the variables x and y as $x = g_1/g_0$ and $y = g_0 + g_1$ and we find the Jacobian determinant [36], which is given by

$$J = -\frac{(1+x)^2}{y}.$$

Thus, the joint *pdf* of x and y can be expressed as follows:

$$\begin{aligned} f_{x,y}(x, y) = {} & \frac{m_s^{m_s} m_{ps}^{m_{ps}} P_p^{-m_{ps}} e^{N_0 B m_{ps}/P_p}}{\Gamma(m_s)\Gamma(m_{ps})} x^{m_s-1}(1+x)^{-m_{ps}-m_s} \\ & \times y^{m_s}(y - N_0 B(1+x))^{m_{ps}-1} \cdot \exp\left\{-y\left(\frac{m_s P_p x + m_{ps}}{P_p(1+x)}\right)\right\} \end{aligned} \tag{32}$$

Integrating $f_{x,y}(x, y)$ with respect to y, we can find the marginal distribution of x, which is given by:

$$\begin{aligned} f_x(x) = {} & \int_{N_0 B(1+x)}^{\infty} f_{x,y}(x, y) dy = \frac{m_s^{m_s} m_{ps}^{m_{ps}} P_p^{-m_{ps}} e^{N_0 B m_{ps}/P_p}}{\Gamma(m_s)\Gamma(m_{ps})} x^{m_s-1}(1+x)^{-m_{ps}-m_s} \\ & \cdot \int_{N_0 B(1+x)}^{\infty} y^{m_s}(y - N_0 B(1+x))^{m_{ps}-1} \exp\left\{-y\left(\frac{m_s P_p x + m_{ps}}{P_p(1+x)}\right)\right\} dy \end{aligned} \tag{33}$$

Using (4.11) from [15, p.348], we get that

$$f_x(x) = \frac{m_s^{m_s} m_{ps}^{m_{ps}} P_p^{\frac{1+m_s-m_{ps}}{2}} e^{\frac{N_0 B m_{ps}}{P_p}} (N_0 B)^{\frac{m_{ps}+m_s-1}{2}}}{\Gamma(m_s)} x^{m_s-1} (m_s x P_p + m_{ps})^{-\frac{m_s+m_{ps}+1}{2}} \cdot \exp\left\{-\frac{N_0 B(m_s x P_p + m_{ps})}{2P_p}\right\} W\left(\frac{1+m_s-m_{ps}}{2}, \frac{-(m_s+m_{ps})}{2}, \frac{N_0 B(m_s x P_p + m_{ps})}{P_p}\right) \tag{34}$$

where $W(\cdot)$ is the Whitakker function [15, p.1024]. Consequently, the average interference power constraint can be simplified to the following:

$$\begin{aligned} Q_{I,av} = \frac{\Gamma(m_p, m_p h_{out})}{\Gamma(m_p)} \Bigg\{ & P_{max} \int_0^\infty \Bigg(1 - \frac{m_{sp}^{-1}}{\Gamma(m_{sp})} \Gamma\Big(m_{sp}+1, \\ & m_{sp}\lambda_0^{-1} a_{SU} x (P_{max}x+1)^{-(a_{SU}+1)}\Big)\Bigg) f_x(x)dx + \frac{m_{sp}^{-\frac{a_{SU}}{a_{SU}+1}}}{\Gamma(m_{sp})} \left(\frac{\lambda_0}{a_{SU}}\right)^{-\frac{1}{a_{SU}+1}} \\ & \times \int_0^\infty x^{-\frac{a_{SU}}{a_{SU}+1}} \left[\Gamma\left(m_{sp} + \frac{a_{SU}}{a_{SU}+1}, m_{sp}\lambda_0^{-1} a_{SU} x (P_{max}x+1)^{-(a_{SU}+1)}\right)\right. \\ & \left. - \Gamma\left(m_{sp} + \frac{a_{SU}}{a_{SU}+1}, m_{sp}\lambda_0^{-1} a_{SU} x\right)\right] f_x(x)dx \\ & - \frac{m_{sp}^{-1}}{\Gamma(m_{sp})} \int_0^\infty x^{-1} \Big[-\Gamma\left(m_{sp}+1, m_{sp}\lambda_0^{-1} a_{SU} x\right) \\ & + \Gamma\left(m_{sp}+1, m_{sp}\lambda_0^{-1} a_{SU} x (P_{max}x+1)^{-(a_{SU}+1)}\right)\Big] f_x(x)dx \Bigg\} \end{aligned} \tag{35}$$

We must note here that the computation of the infinite integrals can be easily performed due to the decreasing behavior of the integrand functions.

References

1. Liu, K. J. R., & Wang, B. (2010). *Cognitive radio networking and security: A game theoretical view*. Cambridge: Cambridge University Press.
2. Wang, B., & Liu, K. J. R. (Feb. 2011). Advances in cognitive radio networks: A survey. *IEEE Journal of Selected Topics Signal Process*, *5*(1), 5–23.
3. Mitola, J., III, (Nov. 1999). Cognitive radio for flexible mobile multimedia communications. In *Proceedings of IEEE international workshop mobile multimedia communication (MMC), San Diego, CA, USA* (Vol. 1, pp. 3–10).
4. Hossain, E., Niyato, D., & Han, Z. (2009). *Dynamic spectrum access and management in cognitive radio networks*. Cambridge: Cambridge University Press.
5. Javan, M. R., & Sharafat, A. R. (May 2013). Distributed joint resource allocation in primary and cognitive wireless networks. *IEEE Transactions on Communication*, *61*(5), 1708–1719.
6. Xu, D., Feng, Z., & Zhang, P. (2012). Resource allocation for heterogeneous services in multiuser cognitive radio networks. *International Journal of Communication System*. doi:10.1002/dac.2462.

7. Chen, J.-L., Liu, S.-W., Wu, S. L., & Chen, M.-C. (Sept. 2011). Cross-layer and cognitive QoS management system for next-generation networking. *International Journal of Communication Systems*, *24*(9), 1150–1162.
8. Wu, D., & Negi, R. (2003). Effective capacity: A wireless link model for support of quality of service. *IEEE Transactions on Wireless Communication*, *2*(4), 630–643.
9. Tang, J., & Zhang, X. (2007). Quality-of-service driven power and rate adaptation over wireless links. *IEEE Transactions on Wireless Communication*, *6*(8), 3058–3068.
10. Zhang, R. (April 2009). On peak versus average interference power constraints for protecting primary users in cognitive radio networks. *IEEE Transactions on Wireless Communication*, *8*(4), 2112–2120.
11. Farraj, A. K., & Hammad, E. M. (July 2013). Impact of quality of service constraints on the performance of spectrum sharing cognitive users. *Wireless Personal Communications*, *71*(2), 975–985.
12. Goldsmith, A., Jafar, S. A., Maric, I., & Srinivasa, S. (May 2009). Breaking spectrum gridlock with cognitive radios: An information theoretic perspective. *Proceedings of the IEEE*, *97*(5), 894–914.
13. Farraj, A. K., & Miller, S. L. (May 2013). Scheduling in a spectrum-sharing cognitive environment under outage probability constraint. *Wireless Personal Communications*, *70*(2), 785–805.
14. Simon, M. K., & Alouini, M.-S. (2005). *Digital communications over fading channels*. New York: Wiley.
15. Gradshteyn, I. S., & Ryzhik, I. M. (1994). *Table of integrals, series, and products* (5th ed.). San Diego: Academic Press.
16. Jovicic, A., & Viswanath, P. (Sept. 2009). Cognitive radio: An information–theoretic perspective. *IEEE Transactions on Information Theory*, *55*(9), 3945–3958.
17. Zhang, L., Liang, Y.-C., & Xin, Y. (Jan. 2008). Joint beamforming and power allocation for multiple access channels in cognitive radio networks. *IEEE Journal of Selected Areas Communication*, *26*(1), 38–51.
18. Chen, Y., Yu, G., Zhang, Z., Chen, H.-H., & Qiu, P. (July 2008). On cognitive radio networks with opportunistic power control strategies in fading channels. *IEEE Transactions on Wireless Communication*, *7*(7), 2752–2761.
19. Ghasemi, A., & Sousa, E. S. (Feb. 2007). Fundamental limits of spectrum-sharing in fading environments. *IEEE Transactions on Wireless Communication*, *6*(2), 649–658.
20. Chang, C.-S., & Thomas, J. A. (1995). Effective bandwidth in high-speed digital networks. *IEEE Journal of Selected Areas Communication*, *13*, 1091–1100.
21. Qiao, D., Gursoy, M. C., & Velipasalar, S. (Feb. 2013). Effective capacity of two-hop wireless communication systems. *IEEE Transactions on Information Theory*, *59*(2), 873–885.
22. Helmy, A., Musavian, L., & Tho, L. N. (Sept. 2013). Energy-efficient power adaptation over a frequency-selective fading channel with delay and power constraints. *IEEE Transactions on Wireless Communication*, *12*(9), 4529–4541.
23. Vassaki, S., Panagopoulos, A. D., & Constantinou, P. (Jan. 2012). Effective capacity and optimal power allocation for mobile satellite systems and services. *IEEE Communication Letters*, *16*(1), 60–63.
24. Ma, Y., Zhang, H., Yuan, D., & Chen, H.-H. (Dec. 2009). Adaptive power allocation with quality-of-service guarantee in cognitive radio networks. *Computer Communications*, *32*(18), 1975–1982.
25. Musavian, L., & Aissa, S. (March 2010). Effective capacity of delay-constrained cognitive radio in Nakagami fading channels. *IEEE Transactions on Wireless Communication*, *9*(3), 1054–1062.
26. Li, D. (Nov. 2010). Effective capacity limits of cognitive radio networks under peak interference constraint. In *IEEE 12th international conference on communication technology (ICCT '10)* (pp. 218–222, 11–14).
27. Akin, S., & Gursoy, M. C. (Nov. 2010). Effective capacity analysis of cognitive radio channels for quality of service provisioning. *IEEE Transactions on Wireless Communications*, *9*(11), 3354–3364.
28. Vassaki, S., Poulakis, M., Panagopoulos, A. D., & Constantinou, P. (Nov. 2011) Optimal power allocation under QoS constraints in cognitive radio systems. In *IEEE 8th international symposium on wireless communication system (ISWCS '11), Aachen, Germany* (pp. 6–9).
29. Kang, X., Liang, Y.-C., Nallanathan, A., Garg, H. K., & Zhang, R. (Feb. 2009). Optimal power allocation for fading channels in cognitive radio networks: Ergodic capacity and outage capacity. *IEEE Transactions on Wireless Communication*, *8*(2), 940–950.
30. Menon, R., Mackenzie, A., Buehrer, R., & Reed, J. (Oct. 2009). Interference avoidance in networks with distributed receivers. *IEEE Transactions on Communication*, *57*(10), 3078–3091.
31. Boche, H., Naik, S., & Alpcan, T. (May 2011). Characterization of convex and concave resource allocation problems in interference coupled wireless systems. *IEEE Transactions on Signal Processing*, *59*(5), 2382–2394.
32. Kuczma, M. (1985). *An introduction to the theory of functional equations and inequalities*. Warsaw: Polish Scientific Publishers PWN.
33. Goldsmith, A. (2005). *Wireless communications*. Cambridge: Cambridge University Press.
34. Boyd, S., & Vandenberghe, L. (2004). *Convex optimization*. Cambridge: Cambridge Univ. Press.

35. Zeidler, E. (2004). *Oxford users guide to mathematics*. Oxford: Oxford University Press.
36. Papoulis, A., & Pillai, S. U. (2002). *Probability, random variables and stochastic processes* (4th ed.). Boston, MA: McGraw-Hill.

Stavroula Vassaki was born in Athens, Greece, in 1984. She received the Diploma degree in electrical and computer engineering from the National Technical University of Athens (NTUA) in 2006 and the M.Sc. degree in economics and administration of telecommunication networks from the National and Kapodistrian University of Athens in 2008. Since November 2006, she has been an Associate Researcher with the Mobile Radio Communications Laboratory, School of Electrical and Computer Engineering, NTUA. She is currently working toward her Ph.D. degree at NTUA. Her research interests include wireless and satellite communications with emphasis on radio resource management, game theory, optimization theory and cognitive radio networks. She has been a Member of the Technical Chamber of Greece since 2007.

Marios I. Poulakis was born in Athens, Greece, in 1983. He received the Diploma degree in electrical and computer engineering from the National Technical University of Athens (NTUA), Athens, and the M.Sc. degree in economics and administration of telecommunication networks from the National and Kapodistrian University of Athens, Athens, in 2006 and 2008, respectively. He is currently working toward the Ph.D. degree at NTUA. Since October 2007, he has been an Associate Researcher with the Mobile Radio Communications Laboratory, School of Electrical and Computer Engineering, NTUA, participating in various industry and research-oriented projects, including electromagnetic field and QoS measurements in GSM and UMTS networks and technical reports on electromagnetic emissions of antenna stations. From August 2009 to January 2010 and from April 2010 to January 2011, he was an RF Engineer with the Non-Ionizing Radiation Office, Greek Atomic Energy Commission, Athens. His research interests include wireless and satellite communications with emphasis on radio resource management, optimization theory, cross layer design and cognitive radios. Mr. Poulakis has been a Member of the Technical Chamber of Greece since 2007.

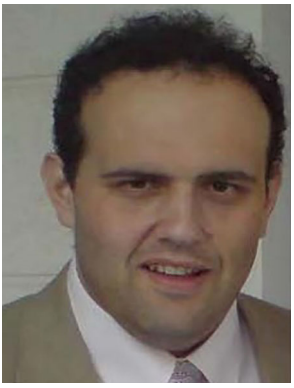

Athanasios D. Panagopoulos was born in Athens, Greece on January 26, 1975. He received the Diploma Degree in Electrical and Computer Engineering (summa cum laude) and the Dr. Engineering Degree from National Technical University of Athens (NTUA) in July 1997 and in April 2002. From May 2002 to July 2003, he served the Technical Corps of Hellenic Army. In September 2003, he joined School of Pedagogical and Technological Education, as part-time Assistant Professor. From January 2005 to May 2008, he was head of the Satellite Division of Hellenic Authority for the Information and Communication Security and Privacy. From May 2008 to October 2013 he was Lecturer in the School of Electrical and Computer Engineering of NTUA and now he is Assistant Professor in the same School. He has published more than 250 papers in international journals (more than 100) and conference proceedings (more than 135), and Book Chapters (more than 15). He is the recipient of URSI General Assembly Young Scientist Award in 2002 and 2005. He is co-recipient of the 3rd place Best Paper Award in the 2006 IEEE Radio and Wireless Symposium. His research interests include radio communication systems design, wireless and satellite communications networks and the propagation effects on multiple access systems and on communication protocols. Since May 2013, he is chairman of Greek Communication Chapter of IEEE. He participates to ITU-R and ETSI Study Groups and he is member of Techni-

cal Chamber of Greece. He serves on the Editorial Boards of the Hindawi International Journal of Antennas and Propagation and International Journal of Vehicular Technology and Elsevier Physical Communication, since October 2008 as an Associate Editor of IEEE Transactions on Antennas and Propagation and since November 2010 as an Associate Editor of IEEE Communication Letters.

Philip Constantinou received the Diploma degree in physics from the National University of Athens (NTUA), Athens, Greece, in 1971, the M.S. degree in applied science from the University of Ottawa, Ottawa, ON, Canada in 1976, and the Dr. Eng. (Ph.D.) degree in electronics from the University of Carleton, Ottawa, in 1983. From 1980 to 1984, he was a Spectrum Engineer and the Head of the Equipment Approval Section, Department of Communications, Ottawa. From 1984 to 1989, he was a Senior Research Scientist on Digital Mobile Communications with the National Center for Scientific Research Demokritos, Athens, Greece. In 1989, he became a Faculty Member with the Department of Electrical and Computer Engineering, NTUA, where he became a Full Professor in 1996 and is currently the Director of the Mobile Radio Communications Laboratory. His research interests include mobile radio communications, mobile satellite and digital communications, radio channel modeling, radio coverage measurements, and interference problems.